PHYSICAL REVIEW A VOLUME 25, NUMBER 3 MARCH 1982

Contribution from close and distant collisions to K-shell excitation in Ge measured using the channeling technique for relativistic protons, π^+, and π^-

J. F. Bak, G. Melchart, and E. Uggerhøj*
CERN, CH-1211 Geneva, Switzerland

J. S. Forster,† P. R. Jensen, H. Madsbøll, S. P. Møller, G. Petersen, and H. E. Schiøtt
Institute of Physics, University of Aarhus, DK-8000 Aarhus C, Denmark

R. Regall and P. Siffert
Centre des Recherches Nucléaires Phase, F-67037 Strasbourg-Cedex, France
(Received 31 August 1981)

For the first time, the impact-parameter dependence for K-shell ionization was measured for relativistic projectiles, although in an indirect way. Experimentally, channeling of GeV projectiles was used to gradually exclude close-encounter processes. In the present experiment, the Lorentz γ factor varied between ~ 2 and ~ 100; in this region, the contribution from distant collisions becomes increasingly important and amounts to about 50% of the total yield for $\gamma \sim 100$. The experimental data are compared to theoretical calculations of impact-parameter distributions, and the agreement is fair for both positive and negative particles.

I. INTRODUCTION

An extensive amount of work, both theoretical and experimental, has been concentrated on understanding inner-shell excitation in the nonrelativistic region.[1] Theoretically, three models have been used to predict cross sections, namely, the plane-wave Born approximation (PWBA),[2] the semiclassical approximation (SCA),[3] and the binary-encounter approximation (BEA).[4,5] It has been shown that straight-line SCA calculations give similar results to those from the PWBA method although they may differ considerably in detail due to different approximations used in the two models. Detailed measurements on differential cross sections have shown that the BEA is unreliable for predicting impact-parameter distributions[6] although total cross sections agree with SCA predictions. To obtain agreement between calculated and measured results, correction terms have been introduced into all calculations to take into account binding effects, Coulomb repulsion, and relativistic effects.

In the relativistic region, most work on inner-shell excitation has been concerned with electron impact. Here reasonable agreement was found between measured and calculated cross sections for energies up to around 1 GeV (for a review, see Ref. 7). However, one puzzling effect was that no density effect was seen although this effect was found in energy-loss measurements. Finally, it is difficult to find a theory that predicts correctly the experimental results over a wide range of targets.[8]

For relativistic heavy particles, little work has been done, especially on the experimental side. Only three sets of data on total cross sections have been reported, one by Jarvis *et al.*[9] (160-MeV/c protons) and two by Anholt *et al.*[10,11] (4.88-GeV/c protons and 3-GeV carbon ions). These experiments were made in order to look for the "relativistic rise" in the cross section stemming from the increased contribution from distant collisions (the current-current interaction). Anholt *et al.*[11] made a partially relativistic PWBA calculation, where the current-current interaction was included, following Fano.[12] They obtained reasonable agreement with experimental total cross sections for $Z \lesssim 40$, but for heavier elements, there was still disagreement. Davidovic *et al.*[13] extended the Møller first-order, time-dependent perturbation theory to relativistic projectile velocities and included relativistic wave functions for the atomic and ejected electrons. Their calculated cross sections agreed satisfactorily over the whole range of targets studied by Anholt *et al.*[11] Recently, Anholt[14] has included a spin-flip term in his calcu-

lations and corrected an error in the previous results. These refined and corrected calculations were also in good agreement with the experimental data over all of the target range.

As in the low-energy region, detailed understanding of the ionization process requires differential cross section studies. Davidovic *et al.*[13] calculated cross sections for GeV protons, but until now, no experimental investigations have been made. Such experiments cannot be performed using low-energy experimental techniques because momentum transfers involved in x-ray excitations correspond to extremely small scattering angles for GeV protons. Such small angles are not detectable, and the scattering process is not well defined. On the other hand, the most direct and sensitive way to measure the increasing influence from distant collisions (the relativistic rise) is via measurements of the impact-parameter dependence of inner-shell excitation. In the GeV region, a classical description of the scattering event is not possible[15]; hence there is no well-defined connection between scattering angles and impact parameters. In channeling, however, which involves a correlated series of collisions, Lindhard[16] demonstrated that a classical description of the scattering process can be applied even though individual scatterings may not be amenable to a classical treatment. Hence a particular incident angle to a crystal axis means a well-defined scattering angle and impact parameter even in the relativistic region. This technique has been used in the present work to measure, for the first time, the impact-parameter dependence of K-shell excitation in germanium.

The ionization probability as a function of impact parameter has been calculated theoretically by Komarov.[17] The cross section was obtained using the BEA for impact parameters less than the K-shell radius a_K and the virual photon approximation for larger impact parameters. More recently, Amundsen and Aashamar[18] extended SCA calculations to the relativistic region. For small impact parameters b ($b \lesssim a_K$), the Komarov results are considerably greater than the SCA calculations, whereas for $b > a_K$, the Komarov results lie around 40% below the SCA results. However, the total cross sections from the two models agree to within 10%.

II. EXPERIMENTAL SETUP

A. General layout

The experimental apparatus was installed in the P17 beam of the CERN 28-GeV/c proton synchroton. A schematic layout of the experiment is shown in Fig. 1. The beam was a high-intensity, secondary, nonseparated, charged beam with momentum adjustable between 2 and 12 GeV/c and had a divergence of ± 1 mrad. Momentum slits allowed reduction of intensity to limits acceptable for the detectors. For the positive projectiles, the beam consisted of roughly equal amounts of protons and pions with about 2% of kaons at 5 GeV/c, whereas for negative projectiles, it contained only pions with 1% antiprotons and kaons.

For each projectile producing and x ray, the experimental equipment recorded the incoming and outgoing angles to the crystals, the x-ray energy, the energy deposited in the crystal, and the time correlation between SC1 and the x-ray detector.

Particle identification was performed in one of two ways: At 2 GeV/c, protons and pions were differentiated by their time of flight (TOF) between SC1 and SC5, the two scintillation counters (SC) placed 16 m apart; for higher momenta, a threshold Cěrenkov counter placed behind SC5 was used. The gas pressure in the Cěrenkov counter was chosen such that a pion or a kaon gave a signal in the counter and a proton no signal.

Two additional scintillation counters, SC3 and SC4, operated in anticoincidence with SC1, SC2, and SC5, defined the usable fraction of the beam

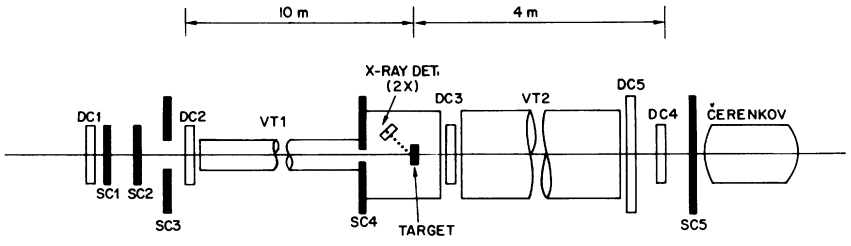

FIG. 1. Schematic drawing of the experimental setup. The beam enters from the left. DC designates drift chamber, SC scintillators, and VT vacuum tubes.

on the crystal sample in the goniometer, placed at the beam focal point.

The incoming and outgoing particle trajectories were measured by a set of five position-sensitive drift chambers, DC1 through DC5. The beam lines VT1 and VT2 were evacuated to a pressure less than 10^{-2} torr, which eliminated contributions to multiple scattering from the air in the tube.

The goniometer allowed adjustment of the crystal axis about the average beam direction although a precise alignment with the beam was not necessary. A liquid-nitrogen cooling system maintained the crystal at a nearly constant temperature of ~ 90 K, and the pressure in the chamber was better than 10^{-2} torr.

B. Drift chambers

For each selected particle track, a series of high-accuracy drift chambers recorded the particle position (x,y) on the selected planes (DC1 – DC5 in Fig. 1). The active area was 150×150 mm^2 for DC1 – DC4 and 500×500 mm^2 for DC5. Drift chamber DC5 was also used to record large scattering angles. The operation of drift chambers has been described elsewhere.[19]

The angular resolution of the system is influenced by two factors, (i) the uncertainty in the drift-chamber coordinates (including the associated electronics) of ~ 0.1 mm, corresponding to an angular uncertainty of ~ 0.02 mrad; (ii) uncertainty in direction due to multiple scattering in the mylar windows and the air gaps close to the crystal. Since DC3 is placed behind the crystal, it produces a small uncertainty in incident-angle measurement, but this is negligible because the distance between crystal and DC3 is only 15 cm, and the multiple scattering in the beam line is 0.05 mrad or less; the uncertainty in position of the projectile on the target is dominated by the uncertainty in the position on DC3. In the present x-ray experiment, only the incident angular resolution is important. It is about 20 μrad and practically independent on projectile momentum.

C. Drift-velocity measurements

To obtain the extremely good angular resolution needed for this experiment, it was necessary to investigate the drift velocity in the drift chambers. In most experiments using drift chambers, the drift velocity v is assumed constant over the entire drift region and to have a value $v = 52.1$ μm/nsec.[19] Since the critical angles for high-energy planar angles are very small (~ 50 μrad), channeling patterns are extremely sensitive to angular resolution. We found that poor transmission-channeling patterns were observed, assuming a constant drift velocity; therefore, an accurate measurement of the drift velocity was made.[20] Two drift chambers were placed in the beam, and the first was fixed and defined a narrow particle beam; the second was placed 175 mm behind the first and could be moved sidewards with a position accuracy of 10 μm. The drift time in the second chamber measured using a TDC having a resolution of 1 nsec. In this way, the total and average drift velocity across the chamber was measured. In Fig. 2 is shown the mean velocity as a function of distance between the particle trajectory and the anode wire. The velocity is seen to have small local variations with an overall decrease in velocity for increasing distance from the wire. In all of our off-line analysis, the small local variations were neglected, but the deviation from constant velocity was taken into account, assuming a linear dependence for v as a function of x [$(v = 56.22$ μm/nsec -0.09 [μm/nsec(mm)]. This relation was obtained with a drift field somewhat higher than normal.[20] As a result, extremely detailed channeling patterns were found, one of which is shown in Fig. 3. Here is plotted, in incident-angle space, the intensity distribution of 10-GeV/c protons transmitted through a 1-mm thick germanium crystal, having scattering angles smaller than 0.1 mrad. It is seen that even high-order crystal planes stand out clearly, the angular widths of which are ~ 50 μrad.

The data acquisition was carried out as described in Ref. 21. In short, for each accepted event, the

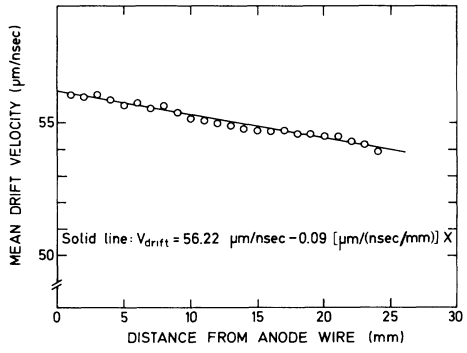

FIG. 2. Variation of mean drift velocity with distance from the anode wire in a drift chamber.

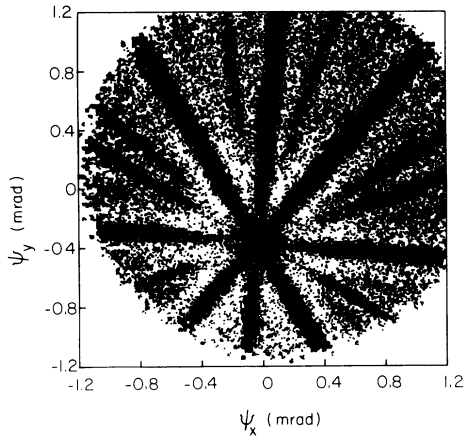

FIG. 3. Stereogram of ⟨110⟩-oriented Ge crystal. The number of projectiles in the two-dimensional angle space of the incident beam, which has been scattered less than 0.1 mrad, is plotted, normalized to the beam intensity. The highest intensity is represented by the darkest area. The axis and planes are very pronounced as multiple scattering is strongly reduced for these projectiles.

output from the drift chambers, the crystal detector, the x-ray detectors, the time correlation between x ray and SC1, and the Čerenkov counters, viz., the TOF measurements, were stored on magnetic tape. The CDC 7600 computer at CERN was used for the full data analysis, while a small on-line computer ensured correct behavior of the detecting system.

D. Preparation of crystal detectors

Few elements form crystals suited for channeling experiments because the critical angles are so small that even a moderate mosaic spread will smear channeling effects. In the present experiment, we have used germanium crystals, which can be produced with very low mosaic spread and are well suited for fabrication of solid-state ionization detectors.

A slight bending of the crystal also leads to a smearing of channeling effect, and special crystal holders were constructed so that the crystals were held without stress being applied. The crystals were checked at room temperature with a double-crystal x-ray spectrometer. From the rocking curve, and accurate measurement of the bendng was obtained. X-ray topography was also employed. In this way, it was ensured that the crystals were bent no more than 10^{-2} mrad. During the experiment, a final test on the crystal bending by means of the transmission effect (cf. Fig. 3) was made. It should be noted that without these predictions, it is not uncommon for samples to be bent as much as 5 mrad.

In order that the germanium crystals could be used as pulse-height detectors, they were prepared in the following way: High-purity n-type material was used with a net impurity concentration below $2.5\times10^{10}/\text{cm}^3$. Samples of various thicknesses (from 0.3 to 4.2 mm), with the ⟨110⟩ axis perpendicular to the surface, were used. The front contact was made by low-energy implantation of boron ions, and a 200-Å aluminum layer was deposited as a back contact. With no heating of the sample, this procedure ensured that the bulk of the material maintained its quality. Cooling of the sample was necessary only during experiments.[21]

The detector electronics was energy calibrated using a ^{133}Ba source. The crystals were aligned with the ⟨110⟩ axis in the middle of the beam cone, using the low-energy—loss method.[22] The alignment was checked by off-line computer analysis, the result of which is shown in Fig. 3.

E. X-ray detector

X-ray detection was performed by two 3-mm thick Si(Li) detectors, each with an active area of ~1 cm^2 placed about 3 cm in front of the target at an angle of 45° to the beam direction. The detectors were mounted in a separate, closed vacuum system and kept at 77 K. The entrance window was 0.1-mm thick Be. Since the P17 beam halo has the same intensity as the main beam, the Si(Li) detectors were hit by primary projectiles, which deposited around 2 MeV during passage. As the electronic amplifiers were set for counting 10-keV x rays, these halo particles caused saturation in the amplifiers. A preamplifier with pulsed optical feedback[23] ensured fast recovery from such pulses. The energy resolution of each detector was about 400 eV at 10 keV. The time correlation between the x-ray detector and SC1 was used to differentiate between real and random events. A window (70 ns) around the x-ray peak in the time spectrum drastically reduced the background, as can be seen in Fig. 4.

F. Effective target thickness, background, and reproducibility

The effective target thickness for the 9.8—keV $K\alpha$ x rays in germanium is determined by self-

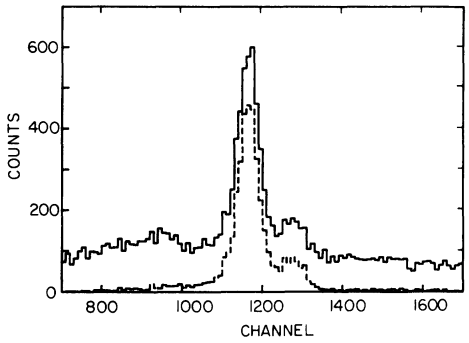

FIG. 4. Spectrum from one of the x-ray detectors for 2.0-GeV/c protons and π^+ on 1.5-mm Ge. Solid line: spectrum with time selection; dashed line: spectrum without time selection (see text).

absorption in germanium, which is $\sim 50\ \mu$m. In the present experiment, the "live" targets were implanted and annealed so that surface effects only influenced the first 1000 Å or less, which was negligible. The random contribution from the channeling surface peak was also negligible since it amounted to less than $\frac{1}{2}\mu$m.

Most background photons around 10 keV are produced by δ electrons. These electrons are ejected from the target by primary projectiles and can, in turn, excite K-shell electrons in the germanium target; also these δ electrons produce bremsstrahlung radiation in the target and surroundings. We have estimated the yield of $K\alpha$ x rays by electron excitation to be at most $5-10\%$ of the yield for an amorphous target. Further, for positive, axially channeled projectiles, the δ-electron yield is reduced to about 15% of normal yield.[24] Thus the x-ray background from the δ electrons is small, especially for channeling directions. The background for bremsstrahlung has also been estimated for an amorphous target and should amount to only about 0.5% and shows a strong directional dependence, which can be seen in Fig. 5. Here is plotted the x-ray background for photon energies between 4 and 8 keV as a function of projectile angle to the ⟨110⟩ axis. The strong influence of channeling is clearly seen.

The x-ray experiment ran for approximately two months although it was interrupted for other measurements. Data from the first and last parts were taken from different targets. Figures 6(a) and 7(a) show results from a 4-mm and a 1.5-mm germanium crystal, and the reproducibility is seen to be good.

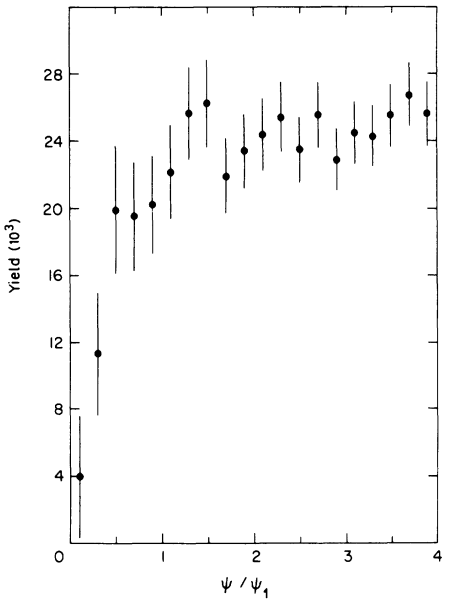

FIG. 5. Scan of incident angles relative to the axis of the normalized-background yield. The background corresponds to x-ray energies between 4 and 8 keV.

III. RESULTS AND DISCUSSION

A. Positive particles. Axial case

Figures 6 and 7 show the x-ray yield for scans through the ⟨110⟩ axis for 2-, 5-, and 12-GeV/c protons and π^+. For comparison, the wide-angle scattering dip for 15-GeV/c protons channeled along a ⟨110⟩ axis is shown in Fig. 8. The channeling dips are plotted as a function of angle between the incident-beam direction and the ⟨110⟩ direction. All curves are normalized to random value (x-ray yield obtained far from crystal axes and planes). The wide-angle scattering dip (Fig. 8) is used for comparison since it shows the influence of channeling on very close-encounter processes. It can be seen that the yield is reduced to a few percent of random when positive particles are incident along axial directions. For the x-ray-yield curves, the background is subtracted using a straight-line approximation underneath the x-ray peak. The minimum in x-ray yield varies from approximately 7% (2-GeV/c protons) to approximately 50% (12-GeV/c π^+) of random, reflecting the increasing influence of distant collisions on K-shell excitation. The values of the γ factor are shown in the plots.

Detailed discussions of channeling may be found in Ref. 16 and in, e.g., Refs. 21, 22, 25, and 26. A

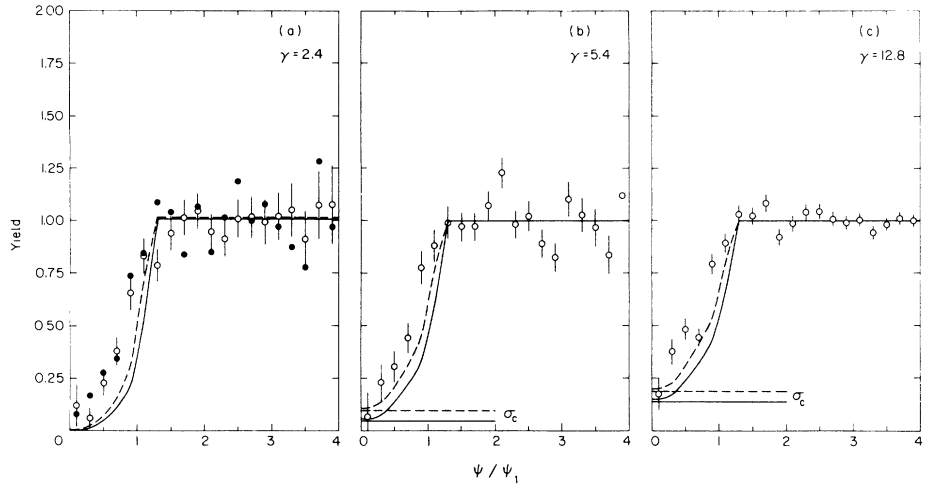

FIG. 6. Measured and calculated channeling dips for K-shell excitation by protons on Ge. The calculated dips are based on the Komarov (Ref. 17) calculations (solid line) and those of Amundsen and Aashamar (Ref. 18) (dashed line). All points shown as open circles have been obtained on the same crystal. The closed circles in (a) were measured on another Ge target. The experimental uncertainties on these points are comparable to the data set shown as open circles. Data for three momenta are shown: (a) 2 GeV/c; (b) 5 GeV/c; (c) 11.9 GeV/c.

discussion of the influence of channeling on inner-shell x-ray yields for nonrelativistic particles may be found in, e.g., Ref. 27. In the following, we give a brief account of the theoretical model employed in the present analysis.

Directional effects for nonrelativistic, positive particles penetrating single crystals have been described theoretically by Lindhard.[16] In his theory, the main concept of an axial row of atoms or atomic strings is introduced. When a particle enters a crystal at a small angle relative to the string, the correlation between successive collisions with the atoms in the string causes the particle to be gently steered away from the string. Consequently, the yield of processes requiring small impact parameters is expected to be strongly reduced compared to the case for an amorphous medium. In a first approximation, the atomic string may be

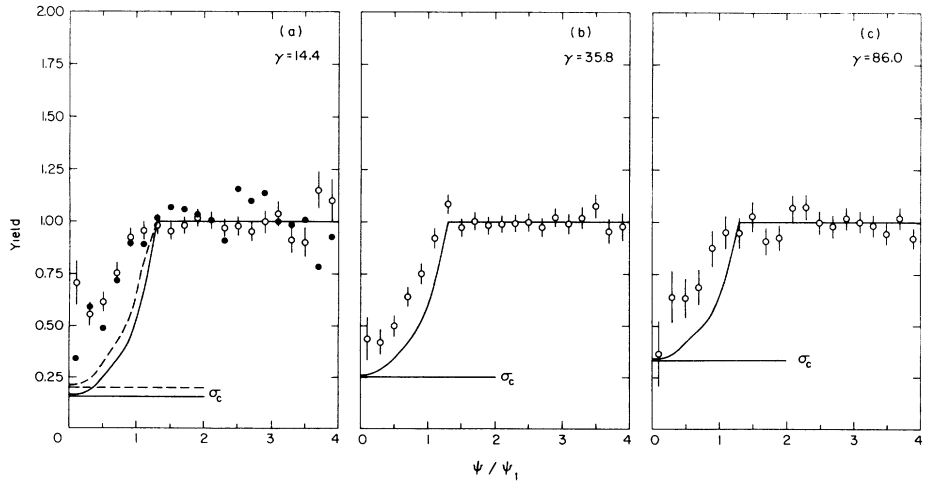

FIG. 7. Same as Fig. 6, but for π^+.

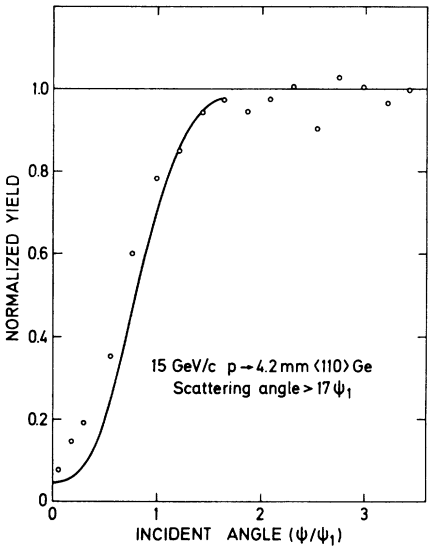

FIG. 8. Comparison between measured and calculated channeling dips for wide-angle scattering of 15-GeV/c protons on Ge. The yield is normalized to random. The theoretical curve, which is based on the modified standard potential, takes into account dechanneling and angular resolution.

described by a continuum potential,

$$U(r)=\int_{-\infty}^{\infty}\frac{dz}{d}V[(z^2+r^2)^{1/2}] ,$$

where r is the distance from the string, $V(R)$ is the ion-atom potential, and d is the distance between atoms in the string. The quantity $U(r)$ plays the role of potential energy for the transverse motion of the particle, i.e., the motion projected onto a plane perpendicular to the string direction. The basic quantity determining the conditions, under which channeling effects occur for small impact-parameter processes, is given by ψ_1,

$$\psi_1=\left[\frac{4Z_1Z_2e^2}{pv\,d}\right]^{1/2} ,$$

where Z_1 and Z_2 are the atomic numbers of the incident particle and the target atoms, respectively, p and v are the relativistic momentum and velocity of the projectile, and d is the distance between target atoms along the string. For low-energy particles, the continuum picture breaks down for incident angles to the crystal axis larger than ψ_1, but in the GeV region, the continuum picture holds for incident angles much larger than ψ_1 (Ref. 25), which means that for high-energy channeling, most calculations can be performed in this simple continuum model. For 12-GeV/c pions, $\psi_1=0.2$ mrad.

The application of a classical orbital picture has been discussed in detail by Lindhard.[16] For a pure Coulomb potential and small scattering angles, Bohr[15] showed that a well-defined classical orbit can be expected if

$$\kappa=R_0/\lambda=2Z_1Z_2e^2/hv>>1 ,$$

where R_0 is the collision diameter and λ is the de Broglie wavelength of the projectile. The Bohr condition may be applied to the transverse plane, which means that

$$R_0\rightarrow a$$

(for $\psi\sim\psi_1$), and

$$\lambda\rightarrow\lambda_\perp=h/p_\perp=h/p\psi_1 .$$

Hence, according to the Bohr condition,

$$\kappa_\perp=a/\lambda_\perp=2\left[\frac{\gamma M_1}{m_0}Z_2^{1/3}Z_1\frac{a_0}{d}\right]^{1/2}>1 ,$$

where $\gamma M_1/m_0$ is the ratio between the projectile mass and the electron rest mass. Clearly, $\kappa_\perp>>1$ for all particles heavier than the electron. Further, $\kappa_\perp$ increases with particle energy because of the appearance of the mass γM_1.

Upon entering the crystal, the particle acquires a transverse energy $E_\perp$ given by

$$E_\perp=\tfrac{1}{2}pv\psi_{\rm in}^2+U(r_{\rm in}) , \quad (1)$$

where $\psi_{\rm in}$ is the angle to the crystal axis and $r_{\rm in}$ is the distance to the axis at the point of entry. In first approximation, this transverse energy is conserved. Because of the stochastic nature of $r_{\rm in}$, there will be a distribution $g(E_\perp,\psi_{\rm in})$ in transverse energies for a beam incident at an angle $\psi_{\rm in}$.

In the present paper, we use a modified Lindhard standard potential,

$$U(r)=\frac{Z_1Z_2e^2}{d}\ln\left[1+\frac{C^2a^2}{r^2+\rho^2}\right] , \quad (2)$$

where a is the Thomas-Fermi screening distance $a\simeq a_0/Z_2^{1/3}$, a_0 is the Bohr radius, C^2 is a constant of the order of three, and ρ^2 is the mean-square thermal-vibrational amplitude of string atoms, perpendicular to the string. This potential approximates the thermally averaged atomic string potential rather well.[28]

Clearly, a channeled particle with transverse energy $E_\perp$ cannot approach the axis closer than a distance $r_{\rm min}$, given by $E_\perp=U(r_{\rm min})$. For such a particle, the impact parameter is $b\geq r_{\rm min}$. With in-

creasing transverse energy, $r_{\min}$ decreases and, for a transverse energy corresponding to an incident angle $\psi_{in} \simeq \psi_1$, the particle is allowed anywhere in the transverse plane. Therefore, for increasing incident angles, still smaller impact parameters contribute to the x-ray yield, and when $\psi_{in} \gtrsim \psi_1$, the same yield as for a random medium is expected.

The yield $\chi(\psi_{in})$ may be calculated from

$$\chi(\psi_{in}) = \int g(E_\perp, \psi_{in}) \pi_{in}(E_\perp) dE_\perp , \quad (3)$$

where $g(E_\perp, \psi_{in})$ is the distribution in transverse energy $E_\perp$ for a given ψ_{in}, and $\pi_{in}(E_\perp)$ is the probability (normalized to random) for a K-shell excitation for a particle of transverse energy $E_\perp$. $\pi_{in}(E_\perp)$ is for the static string given by

$$\pi_{in}(E_\perp) = \frac{A_0}{A(E_\perp)} \frac{\sigma(b > r_{\min})}{\sigma_{tot}} , \quad (4)$$

where A_0 is the total area in the transverse plane belonging to one atomic string and $A(E_\perp)$ is the area available to a particle of transverse energy $E_\perp$. This "area factor" is only slightly above unity. σ_{tot} and $\sigma(b > r_{\min})$ are the total cross section, and the cross section for impact parameters b greater than $r_{\min}(E_\perp)$.

Strictly speaking, the transverse energy is not exactly conserved. Because of scattering on electrons, and, for particles with transverse energy close to $\frac{1}{2} pv\psi_1^2$, on thermally vibrating atoms, the distribution in $E_\perp$ will gradually change with depth. In the present case, however, only ~ 50 μm of the crystal is responsible for K x rays, and we can assume conservation of transverse energy and use the distribution function $g(E_\perp, \psi_{in})$ calculated just inside the crystal surface.[22]

The ionization probability $P(b)$ has been obtained from the calculations of Komarov[17] and of Amundsen and Aashamar.[18] In the Komarov calculations, the cross section is found by using a BEA formalism for b smaller than the radius of the K shell. For $b \geq a$ is used the virtual photon model developed by Willliams and Weizäcker for nuclear and atomic processes. Amundsen and Aashamar[18] have used SCA calculations but extrapolated to relativistic projectiles. The transition amplitude is calculated using first-order, time-dependent perturbation theory, where all multipole contributions are included. Also relativistic K-shell wave functions are included.

In Fig. 9, the two calculations for $P(b)$ are compared for 2-GeV/c protons on germanium. The disagreement for large impact parameters is probably due to the fact that Komarov uses hydrogenic

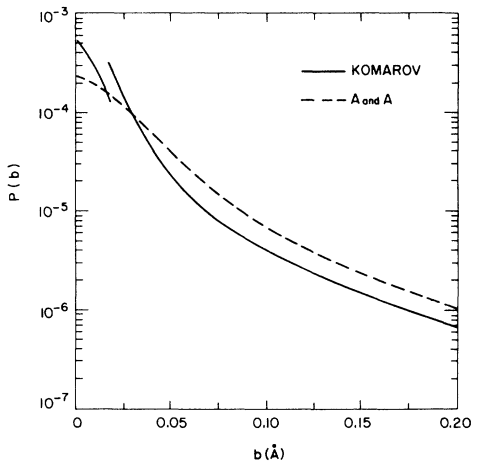

FIG. 9. Impact-parameter distribution of K-shell ionization probability for 2-GeV/c protons on Ge. Solid line: $P(b)$ from Komarov (Ref. 17). The discontinuity at a_K is due to the nonrealistic sharp cutoff of the distant contribution. The discontinuity is of minor importance in channeling calculations. Dashed line: $P(b)$ from Amundsen and Aashamar (Ref. 18).

wave functions without any corrections for outer screening, which even in nonrelativistic collisions underestimates the ionization probability for large impact parameters.[18] For the small impact-parameter part of the Komarov curve, we have used his curve based on the BEA. When the cross sections $P(b)$ are introduced in Eq. (4) and the channeling dips calculated numerically according to Eq. (3), the theoretical curves in Figs. 6 and 7 are obtained.

The minimum yield for particles of low transverse energy increases with increasing γ. It is obvious that this increase is due to the increasing contribution from large impact parameters. By a horizontal line in the plots is indicated the yield obtained for impact parameters larger than 0.5 Å, which seems to give an accurate estimate of the theoretical minimum yield.

In the calculations, the incident beam was assumed to be parallel. As mentioned earlier, we have an angular uncertainty in the incident beam of $\simeq 20$ μrad, but this width is much less than ψ_1 and will not affect the width or the minimum yield of the calculated curves. It is known from drift-chamber measurements that the position distribution is not a true Gaussian but has tails, which can contain up to a few percent of the particles. These tails affect the calculated yield curves by raising the minimum the same few percent. This effect was not taken into account in the curves in Figs. 6

and 7.

Amundsen and Aashamar[18] do not give results for the highest γ values, i.e., corresponding to Figs. 7(b)—7(c). Before discussing the agreement between measured and calculated results, we compare experiment and theory for the channeling case of wide-angle scattering, which is shown in Fig. 8. For such a process, the yield under channeling conditions can be calculated as shown above if the π_{in} function for wide-angle scattering is introduced into Eq. (3). The calculated curve in Fig. 8 was obtained using

$$\pi_{\text{in}}(E_\perp)=\begin{cases}\displaystyle\int_{r_{\min}}^{r_0} e^{-r^2/\rho^2}\frac{dr^2}{\rho^2} & \text{if } E_\perp<E_\perp(\rho)\\ 1, & \text{otherwise,}\end{cases}$$

where $E_\perp(\rho)$ is the transverse energy corresponding to the root-mean-square vibrational amplitude perpendicular to the string, and $r_{\min}$ is found from Eq. (2). In Fig. 8 it is seen that channeling describes reasonably well close-encounter processes. In our experiments on δ-electron emission,[24] we find excellent agreement between experiment and the present simple theoretical description, showing that the model can satisfactorily describe processes (i.e., collisions with electrons), which occur far from the atomic nuclei. In general, there is fair agreement between experimental and theoretical curves, with Amundsen and Aashamar's predictions reproducing better the experimental results than those of Komarov.

The experimental dips are distinctly narrower than the theoretical dips and, especially in the case of pions, the minimum yield is higher than predicted by theory. As mentioned above, the angular resolution may contribute a few percent, and the amorphous surface layer on the crystal will add a contribution estimated to be $\sim 1\%$. When calculating the x-ray yield, we should, in principle, take into account the thermal vibrations of target atoms. As noted by Andersen and Davies,[27] this will increase the mimimum yield by $\sim N d\,\pi\rho^2$, where N is the number of atoms per unit volume. Since this term is $\lesssim 1\%$, we have neglected it in the present context.

As the channeling part of the theoretical calculations seems to be accurate, we believe that the reason for the discrepancy between theory and experiment lies in the inaccuracies in the $P(b)$ curves, where the contribution from distant collisions seems too weak.

B. Planar case

In Fig. 10 is shown the x-ray yield for scans through the (111) and (110) planes. Again, very pronounced dips ($\sim 50\%$) in yield are observed whenever the incident protons and π^+ are aligned with planar directions in the target. Also in the planar case, there is a filling in of the channeling dip between 2-GeV/c protons and 12-GeV/c π^+. This filling in is caused by the increasing contribution to excitation from distant collisions, but the effect is not as pronounced as in the axial case. In the planar case, experimental minumum yields are somewhat high because the incident angular resolution is $\sim\frac{1}{2}\psi_p$, where ψ_p is the planar channeling angle.

C. Negative particles. Axial case

One could try to use the Lindhard classical continuum model to describe channeling phenomena for negative, heavy particles for distances to the string larger than ρ. The difference from the positive case is that a negative beam incident along the axial direction sees an attractive potential $U(r)$ around the crystal axis, resulting in focusing of the beam around the string. For projectiles with angular momentum L to the axis, the effective potential $W(r)$ is

$$W(r)=\frac{L^2}{2M\gamma r}+U(r)\,,$$

which has a minimum for particular values of L.

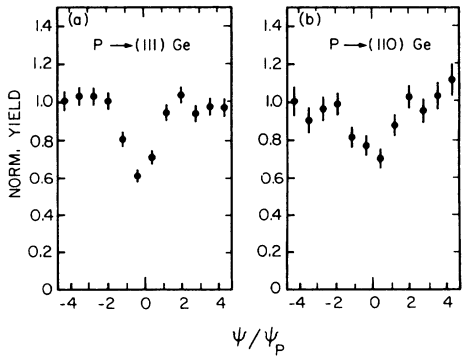

FIG. 10. Scan in incident space across crystalline planes. Normalized yield of x-ray emission from K-shell excitation. Distance to axis greater than $1.5\psi_1$. (a) 11.9-GeV/c protons on (111)Ge (b) 11.9-GeV/c protons on (110)Ge.

Hence a stable spiraling motion becomes possible for certain incident directions. As a net result, negative, channeled particles give increased yields for small incident angles to the string.

Another difference from the positive case, however, is that since those negative particles, which are bound to a particular string, move in a region of space where the density of target atoms is high, the multiple scattering is much stronger than in a random direction, which leads to a rapid dechanneling.[22] Unless the crystal is so thin that dechanneling may be neglected, only few particles will contribute to the increase in yield.

From the present case, we find the width of the Gaussian part of the multiple-scattering distribution for 12-GeV/c negative pions incident on 50-μm amorphous germanium to be ~ 0.07 mrad. For channeled particles, the width is considerably larger and therefore comparable to the critical angle ψ_1 (0.20 mrad). This means that a classical continuum calculation (in which the transverse energy is assumed constant) will give a yield, which is much too high. For positive channeled particles, on the other hand, the multiple scattering is much less than in the random case; dechanneling may be neglected, and a classical continuum calculation is expected to give accurate results.

An alternative method of calculating this yield is to simulate the path of the projectile by means of a series of binary collisions with the crystal atoms. We have made such calculations using Monte-Carlo techniques with a Thomas-Fermi two-body potential and the thermal vibrations of the crystal atoms taken into account. The computer program gives the impact-parameter distribution as a function of distance from the atoms, and this distribution was folded with the impact-parameter dependence of the K-shell ionization predicted by Komarov.[17] Unfortunately, Amundsen and Ashamar[18] do not give predictions for the large γ values. For positive particles, the dip calculated in this way agrees with the standard-model calculations shown in Fig. 7.

Figure 11 shows the experimental x-ray yield (normalized to random) as a function of incident angle to the $\langle 110 \rangle$ germanium axis for 12 GeV/c π^-. Also shown in the figure is the calculated yield curve, using the binary-collision model. Experimentally, a peak in the yield of around 70% over normal yield is found, with a half width at half maximum of $\sim 0.6\psi_1$. The calculated peak is somewhat higher than the experimental results. This might at least partially be explained by the

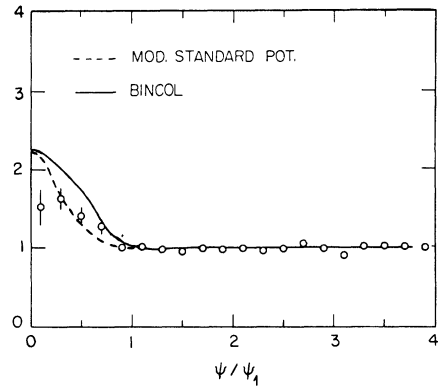

FIG. 11. Same as Fig. 6 but for π^-. Solid line: Yield calculated by folding impact-parameter distribution from binary-collision calculation with $P(b)$ from Komarov (Ref. 17). Dashed line: Continuum calculation, where excess yield is multiplied by 0.25.

fact that the Komarov calculations[17] are systematically higher than the SCA calculations for small impact parameters at lower γ values.

Finally, we show the result of a classical continuum calculation. The calculated excess yield is multiplied by 0.25 in order to approximately account for the effects of dechanneling. A more detailed investigation of the influence of multiple scattering on the excess yield can be found in Ref. 29.

IV. CONCULSION

This work represents the first applicaton of high-energy channeling to vary the impact parameter between projectile and target atom and to study in detail the impact-parameter dependence of K-shell excitation for relativistic projectiles. Based on the theoretical description outlined for MeV particles but transformed to the GeV region, it has been possible to obtain reasonable agreement between calculated and measured x-ray yields for channeled protons and positive pions, with a variation in γ from 2 to 86 and for negative pions, with $\gamma = 86$. For the largest γ values, the contribution from distant collisions becomes increasingly important and accounts for up to $\sim 50\%$ of the contribution to K-shell excitation.

ACKNOWLEDGMENTS

The authors are grateful to the Charpak group at CERN for lending us part of their experimental

setup. S. Kjaer Andersen, Henning Nielsen, and Henry Nielsen are gratefully acknowledged for their participation in the early stages of this experiment. The Danish participation in this collaboration was made possible by funds from the Danish Committee for Accelerator Physics and from the Danish Science Research Council.

---

*Permanent address: Institute of Physics, University of Aarhus, DK-8000 Aarhus C, Denmark.

†Permanent address: Atomic Energy of Canada, Limited, Chalk River Nuclear Laboratories, Chalk River, Ontario, Canada KOJ IJU.

[1]J. D. Garcia, R. J. Fortner, and T. M. Kavanagh, Rev. Mod. Phys. 45, 111 (1973); J. S. Briggs and K. Taulbjerg, *Theory of Inelastic Atom-Atom Collisions,* edited by I. A. Sellin (Springer, Berlin, 1978), Vol. 5, p. 105.

[2]E. Merzbacher and H. Lewis, *Encyclopedia of Physics* (Springer, Berlin, 1958), Vol. 34, p. 166.

[3]J. Bang and J. M. Hansteen, K. Dan. Vidensk. Selsk. Mat. Fys. Medd. 31, No. 31 (1959).

[4]J. D. Garcia, Phys. Rev. A 1, 280 (1970).

[5]J. H. McGuire and P. Richard, Phys. Rev. A 8, 1374 (1973).

[6]E. Laegsgaard, J. U. Andersen, and M. Lund, in *Proceedings of the Tenth ICPEAC, Paris, 1977,* edited by G. Watel (North-Holland, Amsterdam, 1978).

[7]H. Tawara, in *Proceedings of the Tenth ICPEAC, Paris, 1977,* edited by G. Watel (North-Holland, Amsterdam, 1978).

[8]G. R. Dangerfield and B. M. Spicer, J. Phys. B 8, 1744 (1975).

[9]O. N. Jarvis, C. Whitehead, and M. Shah, Phys. Rev. A 5, 1198 (1972).

[10]R. Anholt, S. Nagamiya, J. O. Rasmussen, H. Bowman, J. G. Ioannou-Yannou, and E. Rauscher, Phys. Rev. A 14, 2103 (1976).

[11]R. Anholt, J. G. Ioannou-Yannou, H. Bowman, E. Rauscher, S. Nagamiya, and J. O. Rasmussen, Phys. Lett. 59A, 429 (1977).

[12]U. Fano, Ann. Rev. Nucl. Sci. 13, 1 (1963).

[13]D. M. Davidovic, B. L. Moiseiwitsch, and P. H. Norrington, J. Phys. B 11, 847 (1978).

[14]R. Anholt, Phys. Rev. A 19, 1004 (1979).

[15]N. Bohr, K. Dan. Vidensk. Selsk. Mat. Fys. Medd. 18, No. 8 (1948).

[16]J. Lindhard, K. Dan. Vidensk. Selsk. Mat. Fys. Medd. 34, No. 14 (1965); P. Lervig, J. Lindhard, and V. Nielsen, Nucl. Phys. A96, 481 (1967).

[17]F. F. Komarov, Radiat. Eff. 46, 39 (1980).

[18]P. Amundsen and K. Aashamar, J. Phys. B 14, 4047 (1981).

[19]A. Breskin, G. Charpak, F. Sauli, M. Atkinson, and G. Schultz, Nucl. Instrum. Methods 124, 189 (1975).

[20]J. Bak, P. R. Jensen, H. Madsbøll, S. P. Møller, and E. Uggerhøj (unpublished).

[21]H. Esbensen, O. Fich, J. A. Golovchenko, K. O. Nielsen, E. Uggerhøj, C. Vraast-Thomsen, G. Charpak, S. Majewski, F. Sauli, and J. P. Ponpon, Nucl. Phys. B127, 281 (1977).

[22]S. K. Andersen, O. Fich, H. Nielsen, H. E. Schiøtt, E. Uggerhøj, C. Vraast-Thomsen, G. Charpak, G. Petersen, F. Sauli, J. P. Ponpon, P. Siffert, Nucl. Phys. B167, 1 (1980).

[23]D. Landis, N. Madden, and F. Goulding, IEEE Trans. Nucl. Sci. NS- 26, 428 (1979).

[24]J. Bak, G. Melchart, E. Uggerhøj, J. S. Forster, P. R. Jensen, H. Madsbøll, S. P. Møller, H. Nielsen, G. Petersen, H. E. Schiøtt, R. Regall, and P. Siffert (unpublished).

[25]J. U. Andersen and L. C. Feldman, Phys. Rev. B 1, 2063 (1970).

[26]D. S. Gemmel, Rev. Mod. Phys. 46, 129 (1974).

[27]J. U. Andersen and J. A. Davies, Nucl. Instrum. Methods 132, 179 (1976).

[28]P. R. Jensen, thesis, University of Aarhus, 1980 (unpublished).

[29]S. K. Andersen, F. Bell, F. Frandsen, and E. Uggerhøj, Phys. Rev. B 8, 4913 (1973).